

Horizontal Local Sound Field Propagation Based on Sound Source Dimension Mismatch

Takuma Okamoto

National Institute of Information and Communications Technology
3-5, Hikaridai, Seika-cho, Soraku-gun, Kyoto, 619-0289 Japan
okamoto@nict.go.jp

Received October, 2016; revised January, 2017

ABSTRACT. *This paper provides an analytical method for realizing local sound field propagation that can generate audible acoustic signals close to loudspeakers in the horizontal plane, but very low amplitudes at and beyond the reference distance. The proposed method is based on dimension mismatches between a 3-dimensional sound field propagated from a point source and a sound field produced by a linear sound source. A point source and a linear sound source located close together are produced simultaneously in mutual opposite phase. As a result, the propagated sound pressure at the reference line is completely cancelled, but the propagated sound pressure near the sound source is not compensated. A method using a point source and a linear loudspeaker array is proposed. The driving functions of the sound sources and the produced sound pressures are analytically derived. The results of computer simulations indicate that the proposed method can realize more effective local sound field propagation in the horizontal plane at all of the temporal frequencies than a simple monopole source and the conventional evanescent wave production method.*

Keywords: Local sound field propagation, Sound field control, Loudspeaker array, Spatial Fourier transform, 2.5-dimensional sound field synthesis

1. Introduction. Personalizing a listening area using multiple loudspeakers is an important and attractive sound media enrichment technology since it can transfer sound information to specific users without the use of headphones. In addition, by superposing various localized listening areas, multiple listening zones [1–3] can be generated and they can provide different sound signals at different positions to multi-users. These techniques are useful not only for personal sound systems [4–10] but also for multilingual guide services for multilingual users without headsets. Furthermore, by combining image projection techniques, they can provide different audio-visual contents to different users and are also useful for virtual reality and multimedia applications.

Two approaches to control a sound field using multiple loudspeakers are investigated for personalizing a listening area. Numerous methods have been proposed to control the acoustic contrast or the energy between two spaces [1–3, 5–7, 9–13] and to synthesize multiple sound fields [14–18] using multiple loudspeakers. In these approaches, the control areas are typically set at a distance from loudspeakers.

This paper investigates another approach, where a localized sound area is generated near the loudspeakers so that the produced sound is only propagated near them and the sound energy is quite low at a distance from the loudspeakers. This approach is called local sound field propagation, and several methods have been investigated [19–23].

One is based on evanescent wave [24] synthesis using linear and circular loudspeaker arrays [19, 20]. In these methods, however, the distance attenuation properties at high temporal frequencies are too short, and the listening area becomes too small because the evanescent waves decay in less than one wavelength λ , corresponding to temporal frequency of the produced sound signal [24]¹.

A method using a circular double-layer array [21, 22] is based on the least squares solution which is numerically calculated using control points and loudspeaker positions [5–7, 11, 13–15, 17]. Such methods, however, are quite unstable because the acoustic inverse problem is very ill-conditioned. The ill-conditioning results from the evanescent wave information contained in the decaying pressure of the high spatial wavelength waves which blow up exponentially in the inversion process [24, 25]. To solve the ill-conditioned problem, an analytical approach using a circular double-layer array has been recently investigated [26].

An analytical method based on a linear and circular loudspeaker array combination has been proposed for 3-dimensional local sound field propagation [23]. This method, however, is not suited for actual implementations since the array's configuration is complicated and the audible sound zone is inside a circular array.

For realizing local sound field propagation for a large quiet zone with simple loudspeaker array configurations, this paper provides an analytical approach which is based on dimension mismatch between 3-dimensional sound field propagation by a point source and horizontal sound field synthesis using a linear sound source: 2.5-dimensional sound field synthesis [3, 27–29]. An important restriction exists: it can only synthesize correct sound pressure at a reference line because of sound source dimension mismatch. Two types of sound sources, located close together, are simultaneously produced in mutual opposite phase. The propagated sound pressure at the reference line is completely cancelled, whereas the propagated sound pressure near the sound source is not compensated. The driving functions of the sound sources and the produced sound pressures in the horizontal plane are analytically derived instead of the least squares solution used in previous methods [21, 22]. Compared with the evanescent wave production methods [19, 20] and the method based on a linear and circular array combination [23], the proposed method can realize horizontal local sound field propagation with optimal propagation distance at all temporal frequencies.

The remainder of this paper is organized as follows. Section 2 introduces the basic principles and the properties of a 2.5-dimensional sound field synthesis using a linear sound source. An analytical method for horizontal local sound field propagation using a point source and a linear loudspeaker array is proposed in Section 3. In Section 4, computer simulations were performed to evaluate the proposed method. Finally, Section 5 concludes this paper.

2. 2.5-dimensional sound field synthesis using a linear sound source. For actual implementations, sound field synthesis systems are frequently simplified in the horizontal plane. The sound sources are then arranged in a line or a circle. For 2-dimensional sound field synthesis, the sound sources must be a line source for which the transfer function is defined as a 2-dimensional free-field Green's function. However, in actual implementations, loudspeakers with closed cabinets are generally used instead of line sources. Each loudspeaker is modeled as a point source for which the transfer function is defined as a 3-dimensional free-field Green's function. Due to this sound source dimension mismatch, sound field synthesis using a linear or a circular sound source can only synthesize correct sound pressure at the reference line or circle. Such approaches are designated as

¹The sound pressures both in the temporal and spatial frequency domains are defined in the appendix.

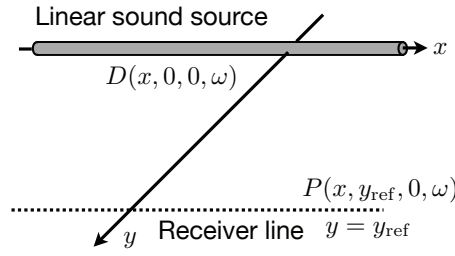


FIGURE 1. 2.5-dimensional sound field synthesis using a linear sound source.

2.5-dimensional sound field synthesis [3, 27–29]. This section describes its basic principles using a linear sound source.

Sound pressure $P(\mathbf{x}, \omega)$, synthesized at position $\mathbf{x} = [x, y, z]^T$ by a continuous linear sound source along the x -axis, is given as

$$P(\mathbf{x}, \omega) = \int_{-\infty}^{\infty} D(\mathbf{x}_0, \omega) G_{3D}(\mathbf{x} - \mathbf{x}_0, \omega) dx_0, \quad (1)$$

where $\omega = 2\pi f$ denotes the radiant frequency, f represents the temporal frequency, $D(\mathbf{x}_0, \omega)$ stands for the sound source driving function at position $\mathbf{x}_0 = [x_0, y_0 = 0, z_0 = 0]^T$, $G_{3D}(\mathbf{x} - \mathbf{x}_0, \omega)$ denotes the transfer function of the sound source placed at \mathbf{x}_0 to point \mathbf{x} , and dx_0 stands for a linear element for integration. Under the free-field assumption, $G_{3D}(\mathbf{x} - \mathbf{x}_0, \omega)$ is the 3-dimensional free-field Green's function [24], defined as

$$G_{3D}(\mathbf{x} - \mathbf{x}_0, \omega) = \frac{e^{-jk|\mathbf{x} - \mathbf{x}_0|}}{4\pi|\mathbf{x} - \mathbf{x}_0|}, \quad (2)$$

where $j = \sqrt{-1}$, $k = \omega/c$ denotes the wavenumber. When applying the spatial Fourier transform [24] to equation (1) with respect to the x -axis, the convolution along it is performed using the convolution theorem:

$$\tilde{P}(k_x, y, z, \omega) = \tilde{D}(k_x, \omega) \tilde{G}(k_x, y, z, \omega), \quad (3)$$

where k_x denotes the spatial frequency in the direction of x and $\tilde{G}(k_x, y, z, \omega)$ is the spatial Fourier transform of $G_{3D}(\mathbf{x} - \mathbf{x}_0, \omega)$ with respect to the x -axis. In the convolution theorem, $x_0 = 0$ and $\tilde{G}(k_x, y, z, \omega)$ is calculated by using (3.876-1) and (3.876-2) in [30] and given as

$$\begin{aligned} \tilde{G}(k_x, y, z, \omega) &= \int_{-\infty}^{\infty} \frac{e^{-jk\sqrt{(x-x_0)^2 + (y-y_0)^2 + (z-z_0)^2}}}{4\pi\sqrt{(x-x_0)^2 + (y-y_0)^2 + (z-z_0)^2}} e^{jk_x(x-x_0)} dx \\ &= \int_{-\infty}^{\infty} \frac{e^{-jk\sqrt{x^2 + y^2 + z^2}}}{4\pi\sqrt{x^2 + y^2 + z^2}} e^{jk_x x} dx = -\frac{j}{4} H_0^{(2)}\left(k_\rho \sqrt{y^2 + z^2}\right), \end{aligned} \quad (4)$$

where $H_0^{(2)}$ denotes the zero-th order Hankel function of the second kind [24] and $k_\rho = \sqrt{k^2 - k_x^2}$.

When the continuous receiver line is located at $y = y_{\text{ref}}$ and $z = 0$ (Figure 1), the sound source driving function in the wavenumber domain is directly derived from equations (3) and (4), given as

$$\tilde{D}(k_x, \omega) = \frac{4j\tilde{P}(k_x, y_{\text{ref}}, 0, \omega)}{H_0^{(2)}(k_\rho y_{\text{ref}})}, \quad (5)$$

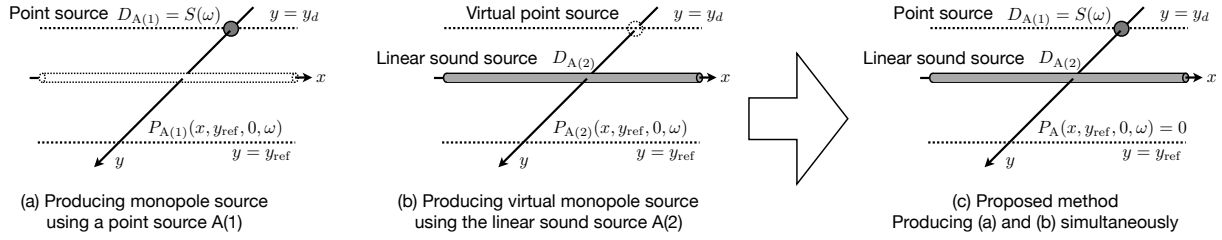


FIGURE 2. Arrangements of sound sources and scheme of proposed method. $D_{A(1)}$ and $D_{A(2)}$ are respective driving functions of point source A(1) given as equation (7) and linear sound source A(2) given as equation (11). $P_{A(1)}$ and $P_{A(2)}$ are sound pressures produced by sound sources A(1) and A(2) defined in equations (9) and (12). P_A is total produced sound pressure in proposed method given in equation (13).

in the spectral division method (SDM) [28]. From equations (3) and (5), the produced sound pressure is then represented:

$$\tilde{P}(k_x, y, 0, \omega) = \frac{\tilde{P}(k_x, y_{ref}, 0, \omega)}{H_0^{(2)}(k_\rho y_{ref})} H_0^{(2)}(k_\rho y). \quad (6)$$

In the SDM using a linear sound source (2.5-dimensional SDM), equation (6) shows that the produced sound pressure is correct only at reference receiver line $y = y_{ref}$ because driving function $\tilde{D}(k_x, \omega)$ is dependent on the reference receiver line [28]. In addition, this property indicates that the propagation property of 2.5-dimensional SDM is different from that of the 3-dimensional sound sources. This property is also found in the wave field synthesis (WFS) using a linear sound source (2.5-dimensional WFS) [27].

3. Proposed method for horizontal local sound field propagation. The following two main properties in 2.5-dimensional sound field synthesis are described in Section 2:

1. The produced sound pressure is correct only at the reference receiver line.
2. The propagation property of the 2.5-dimensional sound field synthesis is different from the 3-dimensional sound sources.

In this section, an analytical method for achieving local sound field propagation in the horizontal plane is proposed based on the radiation property mismatch between a 3-dimensional point source and a sound field produced by a linear loudspeaker array with 2.5-dimensional sound field synthesis.

The fundamental concept of the proposed method is that a 3-dimensional point source and a linear sound source located close together are simultaneously produced in mutual opposite phase. The sound pressure at reference line y_{ref} is set manually [1–3]. Each driving function of each sound source is calculated from equations (5) with y_{ref} . The first property suggests that the sound pressures produced by the two sound sources are completely cancelled out at the reference line. The second property indicates that the produced sound pressure level is only high near the sound source, but it is quite low at $y > y_{ref}$. As a result, local sound field propagation can be realized by the proposed method. The driving functions of the point and linear sound sources and the produced sound pressures in the horizontal plane are analytically derived and analyzed.

Point source A(1) and linear sound source A(2) are located at $\mathbf{x}_s = [0, y_d (< 0), 0]^T$ and along the x -axis. The arrangements of the sound sources and the scheme of the proposed method are shown in Figure 2.

In the first step, the driving function of point source A(1) is set to

$$D_{A(1)}(\omega) = S(\omega), \quad (7)$$

where $S(\omega)$ is the sound source signal. The sound pressure at \mathbf{x} produced by point source A(1) is then obtained:

$$P_{A(1)}(\mathbf{x}, \omega) = S(\omega)G_{3D}(\mathbf{x} - \mathbf{x}_s, \omega) = \frac{S(\omega)e^{-jk|\mathbf{x} - \mathbf{x}_s|}}{4\pi|\mathbf{x} - \mathbf{x}_s|}. \quad (8)$$

From the spatial Fourier transform of equation (8) with respect to the x -axis, the sound pressure on the x - y plane with $y > 0$ produced by point source A(1) in the wavenumber domain is calculated:

$$\tilde{P}_{A(1)}(k_x, y, 0, \omega) = -\frac{j}{4}S(\omega)H_0^{(2)}(k_\rho(y - y_d)). \quad (9)$$

In the second step, we consider a case where a virtual point source is produced using linear sound source A(2) along the x -axis. The driving function of a linear sound source in the wavenumber domain for producing a virtual point source at position $\mathbf{x}_s = [x_d, y_d, 0]^T$ was previously proposed [31]:

$$\tilde{D}_{fs}(k_x, \omega) = S(\omega)e^{jk_x x_d} \frac{\tilde{G}_x(k_x, y_{ref} - y_d, \omega)}{\tilde{G}_x(k_x, y_{ref}, \omega)} = S(\omega)e^{jk_x x_d} \frac{H_0^{(2)}(k_\rho(y_{ref} - y_d))}{H_0^{(2)}(k_\rho y_{ref})}. \quad (10)$$

In the proposed method, $x_d = 0$ and linear sound source A(2) are produced in opposite phases with point source A(1). The driving function of linear sound source A(2) in the wavenumber domain is then represented as

$$\tilde{D}_{A(2)}(k_x, \omega) = -S(\omega) \frac{H_0^{(2)}(k_\rho(y_{ref} - y_d))}{H_0^{(2)}(k_\rho y_{ref})}. \quad (11)$$

The sound pressure in the wavenumber domain produced by linear sound source A(2) is obtained from equations (3) and (11):

$$\tilde{P}_{A(2)}(k_x, y, 0, \omega) = \frac{jS(\omega)H_0^{(2)}(k_\rho(y_{ref} - y_d))}{4H_0^{(2)}(k_\rho y_{ref})} \cdot H_0^{(2)}(k_\rho y). \quad (12)$$

Finally, by simultaneously producing the driving functions in equations (7) and (11), local sound field propagation in the horizontal plane can be achieved. The total produced sound pressure in the wavenumber domain is analytically obtained:

$$\begin{aligned} \tilde{P}_A(k_x, y, 0, \omega) &= \tilde{P}_{A(1)}(k_x, y, 0, \omega) + \tilde{P}_{A(2)}(k_x, y, 0, \omega) \\ &= -\frac{j}{4}S(\omega)H_0^{(2)}(k_\rho(y - y_d)) + \frac{jS(\omega)H_0^{(2)}(k_\rho(y_{ref} - y_d))}{4H_0^{(2)}(k_\rho y_{ref})} H_0^{(2)}(k_\rho y). \end{aligned} \quad (13)$$

For $y = y_{ref}$, $\tilde{P}_A(k_x, y, \omega)$ is exactly 0. In contrast, for $y \neq y_{ref}$, $\tilde{P}_A(k_x, y, \omega) \neq 0$.

Equation (13) indicates that the propagation property of the proposed method is determined by the position of monopole y_d and reference distance y_{ref} . y_{ref} can set the sound field cancellation distance, and the smaller y_{ref} is, the more precipitous the distance attenuation property becomes. When $|y_d|$ is quite small, $\tilde{P}_A(k_x, y, 0, \omega)$ is 0 at almost y and the distance attenuation property also becomes precipitous. On the other hand, when $|y_d|$ is not so small, $\tilde{P}_A(k_x, y, 0, \omega)$ is not 0 at a small y and the distance attenuation property is not so precipitous. These analyses imply that local sound field propagation can be realized by the proposed method.

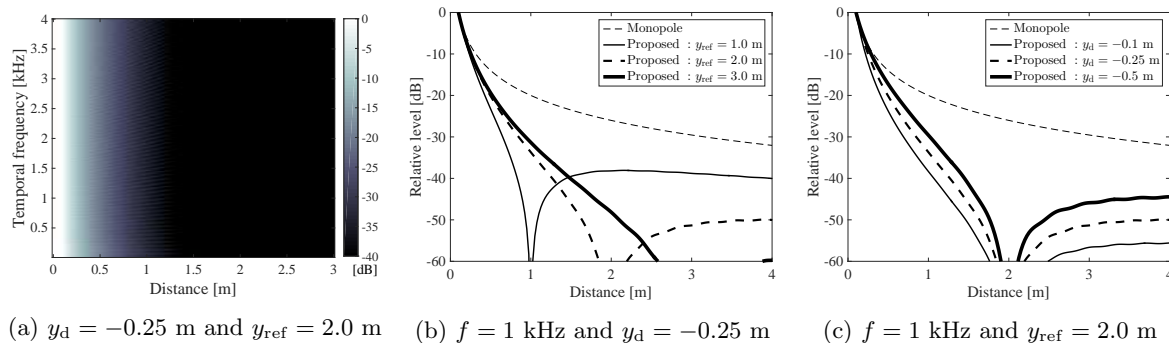


FIGURE 3. Results of theoretical distance attenuation properties of proposed method along with the y -axis: (a) up to $f = 4$ kHz, (B) $y_{\text{ref}} = 1.0$, 2.0 and 3.0 m, and (c) $y_d = -0.1$, -0.25 and -0.5 m.

The driving function of the proposed method in the temporal frequency domain is finally derived by the inverse spatial Fourier transform [24, 28]:

$$D_{A(2)}(x, \omega) = \frac{1}{2\pi} \int_{-\infty}^{\infty} \tilde{D}_{A(2)}(k_x, \omega) e^{-jk_x x} dk_x. \quad (14)$$

For actual implementations, a linear loudspeaker array instead of a continuous linear sound source is used, and equation (14) was discretized and truncated [1–3, 23, 29, 32]. The truncation and discretization properties of the driving function in the SDM have been scrutinized [28]. The effect of the truncation and the discretization of a linear sound source in the proposed method is discussed in Section 4.2.

4. Computer simulations and discussion. Computer simulations evaluated the proposed method. In all the calculations, speed of sound c was 343.26 m/s, the sound source signal $S(\omega) = 1$, and a three-dimensional free-field is assumed.

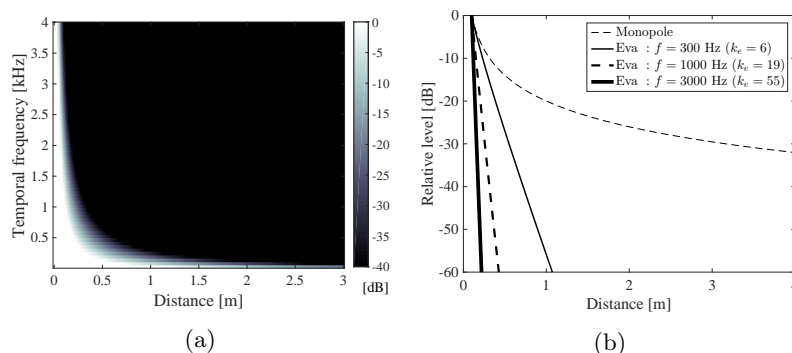


FIGURE 4. Results of theoretical distance attenuation properties of evanescent wave production method using a linear sound source along with the y -axis: (a) up to $f = 4$ kHz, and (B) $f = 300$, 1000 and 3000 Hz.

4.1. Theoretical distance attenuation property. The theoretical distance attenuation property of the proposed method up to $f = 4$ kHz is compared in Figure 3 with a simple monopole source. To compare the theoretical distance attenuation property of the proposed method with that of the conventional evanescent wave production method [19, 20], the theoretical distance attenuation property of the evanescent wave production method using a linear loudspeaker array [19] is also plotted in Figure 4.

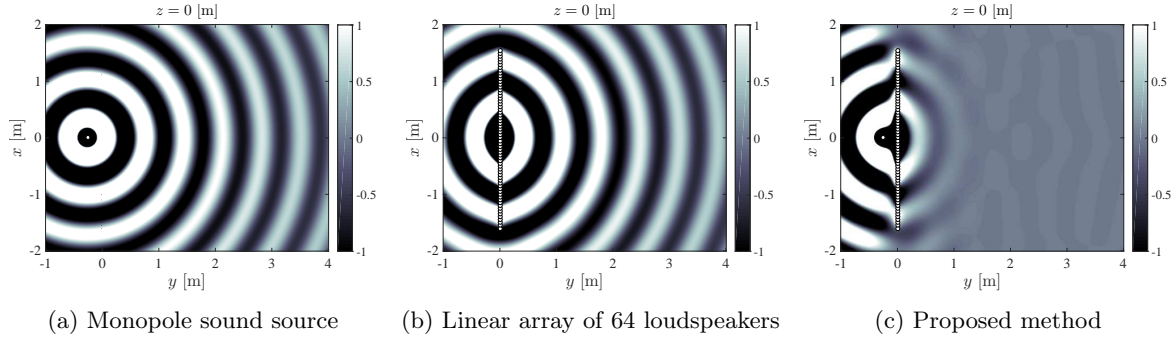


FIGURE 5. Results of propagated sound pressures produced by (a) monopole sound source: $D_{A(1)}$, (b) linear array of 64 loudspeakers: $D_{A(2)}$ and (c) proposed method: $D_{A(1)} + D_{A(2)}$ for $f = 500$ Hz with $\Delta x = 0.05$ m and $y_{\text{ref}} = 2.0$ m. White circles are loudspeakers.

To calculate these results, the produced sound pressures of the proposed method at $x = 0$ m and $0.1 \text{ m} \leq y \leq 4 \text{ m}$ were numerically calculated from the discrete driving signals, and the discretized representation of equations (14) and (1) where f , y_d and y_{ref} were set as:

- Figure 3(a): up to $f = 4$ kHz with $y_d = -0.25$ m and $y_{\text{ref}} = 2.0$ m
- Figure 3(b): $y_{\text{ref}} = 1.0, 2.0$ and 3.0 m with $f = 1.0$ kHz and $y_d = -0.25$ m
- Figure 3(b): $y_d = -0.1, -0.25$ and -0.5 m with $f = 1.0$ kHz and $y_{\text{ref}} = 2.0$ m

The produced sound pressure of the evanescent wave production method using a previously derived linear sound source [19] is given as

$$P_{\text{eva}}(x, y, 0, \omega) = \frac{2\pi e^{-k_e y_{\text{ref}}}}{K_0(k_e y_{\text{ref}})} e^{-j\sqrt{k^2 - k_e^2}x} K_0(k_e |y|), \quad (15)$$

where K_0 denotes the 0-th order modified Bessel function of the second kind [24] and k_e corresponds to the distance attenuation term [19] that must be $k_e > k$ [24]. In Figure 4, k_e was set to $\lceil k \rceil$ at each temporal frequency where $\lceil \cdot \rceil$ is the ceiling function. y_{ref} in equation (15) was set to 2 m, and the produced sound pressure at $x = 0$ m and $0.1 \text{ m} \leq y \leq 4 \text{ m}$ was also calculated.

The theoretical distance attenuation property was calculated as produced sound pressure level $20 \log_{10} |P_{\text{proposed,eva}}|$. In Figures 3 and 4, the distance attenuation property of a simple monopole source was calculated as $20 \log_{10} |e^{-jkr}/4\pi r|$. $20 \log_{10} |P_{\text{proposed,eva}}|$ at $\mathbf{x} = [0, 0.1, 0]^T$ were both set to 0 dB.

The results of Figure 4 suggest that the evanescent wave production method can only control the attenuation property at low temporal frequency ($f = 300$ Hz) with appropriate decay, whereas that at high temporal frequencies ($f = 1$ kHz and 3 kHz) is too precipitous and the listening area becomes too small, because the evanescent wave decays less than one wavelength, which corresponds to the produced sound's temporal frequency, and k_e in equation (15) must be $k_e > k$ [24]. In contrast, the results from Figure 3 indicate that the proposed method can achieve more effective local sound field propagation with appropriate decay at all of the temporal frequencies compared with the evanescent wave production method and a simple monopole source.

The result of Figure 3(b) shows that the produced sound pressure is completely cancelled at set reference line y_{ref} . If y_{ref} is small ($= 1$ m), the distance attenuation property is precipitous, but the produced sound pressure level at $y > y_{\text{ref}}$ is increased again because the distance attenuation properties between sound sources A(1) and A(2) are quite different. y_{ref} must be set to an optimal value ($= 2$ or 3 m).

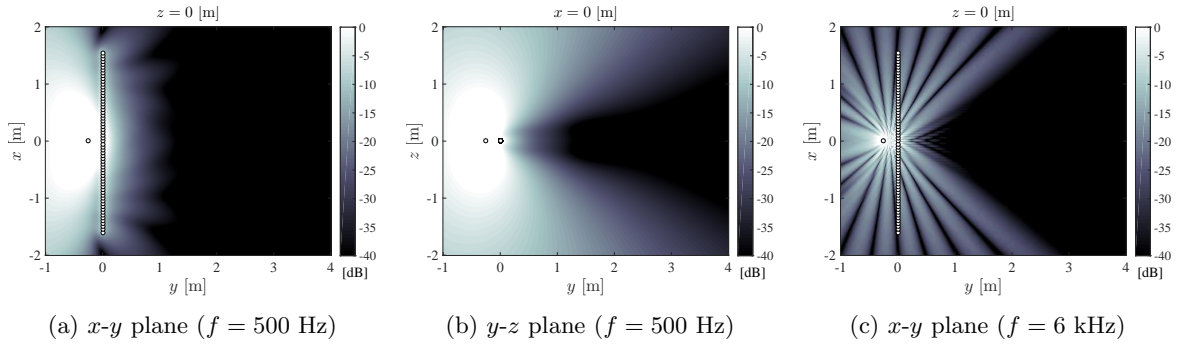


FIGURE 6. Results of sound pressure level produced by proposed method using linear array of 64 loudspeakers with $\Delta x = 0.05$ m and $y_{\text{ref}} = 2.0$ m. Produced sound pressure level at $\mathbf{x} = [0, 0.1, 0]^T$ is set to 0 dB. White circles are loudspeakers.

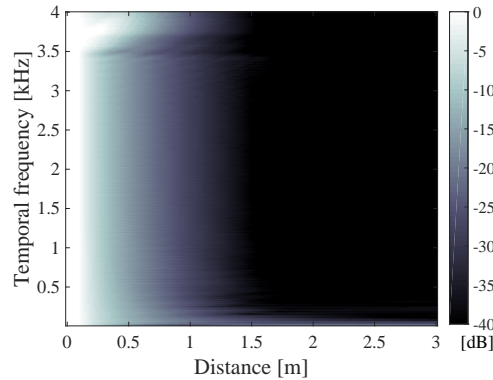


FIGURE 7. Results of distance amplitude properties for proposed method using a linear array of 64 loudspeakers with $\Delta x = 0.05$ m and $y_{\text{ref}} = 2$ m calculated from produced sound pressure level $20 \log_{10} |P_A|$ along with y -axis to $f = 4$ kHz. Spatial Nyquist frequencies of proposed method is about 3.4 kHz.

As described in Section 3, the result of Figure 3(c) indicates that y_d can slightly control the distance attenuation property and that smaller $|y_d|$ is better for reducing the produced sound pressure level at $y > y_{\text{ref}}$.

4.2. Actual implementations using a linear loudspeaker array. For practical implementations, a linear loudspeaker array is introduced instead of a continuous linear sound source distribution.

In the simulations for the proposed method with a linear loudspeaker array, a discretized and truncated linear array of 64 loudspeakers was used with distance between the adjacent loudspeakers $\Delta x = 0.05$ m. This linear array's spatial Nyquist frequency was about 3.4 kHz. Equation (14) was discretized as $dk_x \rightarrow \Delta k_x = 0.5$ and truncated to $-\pi/\Delta x \leq k_x \leq \pi/\Delta x$.

Figure 5 shows the results of the propagated sound pressures on the horizontal plane produced by point source A(1), a discretized linear array of 64 loudspeakers A(2), and the proposed method with $y_d = -0.25$ m and $y_{\text{ref}} = 2.0$ m for $f = 500$ Hz. Figure 6 shows the result of the sound pressure level produced by the proposed method with a linear array of 64 loudspeakers. In addition, Figure 7 shows the result of the distance attenuation properties of the proposed method with the linear array along the y -axis to $f = 4$ kHz.

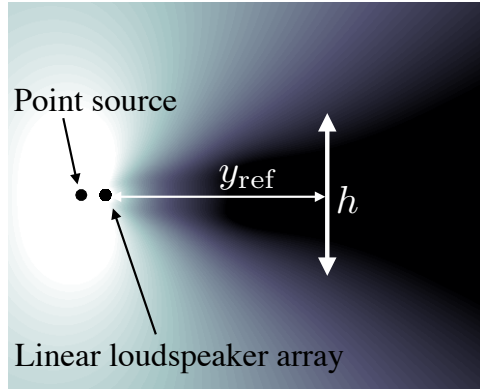


FIGURE 8. Definition of possible height of quiet zone as maximum h for which $BDR(\omega)$ between bright position $\mathbf{x}_b = [0, y_b, 0]^T$ and quiet zone $\mathbf{x}_q = [0, y_q, -h/2 \leq z \leq h/2]^T$ remains above 40 dB.

The results in Figures 5, 6(a), and 7 show that optimal local sound field propagation in the horizontal plane can be realized by the proposed method within spatial Nyquist frequency. When f exceeded the spatial Nyquist frequency, spatial aliasing occurred, as shown in Figures 6(c) and 7. The results of Figures 5, 6(a) and 7 suggest that the truncation of the linear array is less problematic for realizing local sound field propagation along with the y -axis. However, the result of Figure 7 suggests that the proposed method with a truncated linear array cannot be controlled at lower frequencies (less than 100 Hz) because of the truncation error where the wavelength is longer than the truncated array and $\tilde{D}_{A(2)}(k_x, \omega)$ around $k_x = k/2$ cannot be synthesized correctly.

The driving signal and the synthesized sound field by the linear array are also used in the next subsections for detailed analyses.

4.3. Radiation to vertical angles and possible shape of quiet zone. The driving function and the produced sound pressure of the proposed method are derived only on the x - y plane; the z -axis is not considered at all. In actual environments, however, the produced sound pressure is radiated in all directions. The result of the sound pressure level radiated by the proposed method for $f = 500$ Hz on the y - z plane is shown in Figure 6(b). Similar to the conventional method using circular double-layer array [21,22], this result suggests that the undesired sound pressures are radiated to the vertical angles.

If the radiation to the vertical angles is severe, the proposed approach cannot be used in actual implementations. To estimate the availability of the proposed method for actual implementations, the possible height of the quiet zone was investigated because no evaluation was previously conducted [21,22]. To evaluate the quiet zone's possible height, the bright to dark ratio $BDR(\omega)$, which is the sound pressure level between bright position \mathbf{x}_b and quiet zone \mathbf{x}_q [1–3], was first defined as

$$BDR(\omega) = 20 \log_{10} \frac{|P(\mathbf{x}_b)|}{|P(\mathbf{x}_q)| / \int d\mathbf{x}_q}. \quad (16)$$

As shown in Figure 8, the possible height of the quiet zone was defined as maximum height h for which $BDR(\omega)$ between bright position $\mathbf{x}_b = [0, y_b, 0]^T$ and quiet zone $\mathbf{x}_q = [0, y_q, -h/2 \leq z \leq h/2]^T$ remains above 40 dB.

If $|y_d|$ in the proposed method is large, the radiation properties between a monopole source and a linear loudspeaker array are quite different, and only the sound pressures radiated in the horizontal plane are cancelled. When $|y_d|$ is small, on the other hand, these radiation properties might become similar and the sound pressures radiated to the

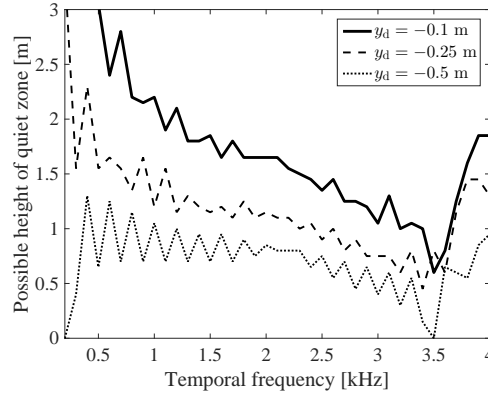


FIGURE 9. Results of possible heights of quiet zone h for proposed method with linear array of 64 loudspeakers.

vertical angles might also be cancelled. To enlarge the possible height of the quiet zone, therefore, the smaller $|y_d|$ is, the larger the quiet zone is.

The possible height of quiet zone h of the proposed method was calculated where y_d was -0.1 , -0.25 , and -0.5 m, $y_b = 0.1$ m and $y_q = y_{\text{ref}} = 2.0$ m. As a reference, $BDR(\omega)$ of a simple monopole at the origin between $\mathbf{x}_b = [0, 0.1, 0]^T$ and $\mathbf{x}_q = [0, 2.0, 0]^T$ was about 26 dB.

Figure 9 shows the result of the possible height of quiet zone h . The result suggests that the hypothesis is valid and that $|y_d|$ should be as small as possible to expand the quiet zone. The proposed method with $y_d -0.1$ m, where the distance between the adjacent loudspeakers is also about 0.05 m, can realize local sound field propagation with possible height of quiet zone h of about 1.0 m. The result indicates the practical aspect of the proposed method for multiple users of different heights.

4.4. Stability of driving signals and frequency responses of produced sound field. To evaluate the efficiency of the proposed system, the stability of the driving signals and the frequency responses of the produced sound field were investigated.

We compared the stability of the driving signals as the required energy analysis of linear loudspeaker arrays to a monopole sound source. The required energy of a linear loudspeaker array at each temporal frequency was evaluated as

$$E_A = 20 \log_{10} \frac{\left| \int D_{A(2)}(\mathbf{x}_0, \omega) d\mathbf{x}_0 \right|}{\left| D_{A(1)}(\omega) \right|}. \quad (17)$$

The results of required energy E_A of the driving signals calculated in Section 4.2 were plotted in Figure 10, where $20 \log_{10} |D_{A(1)}(\omega)|$ was just 0 dB. They were about -12 to -0.2 dB and stable at each temporal frequency.

We also calculated the frequency responses at two listening positions ($[0, 0.5, 0]^T$ and $[1, 0.5, 0]^T$) and two quiet positions ($[0, 2.5, 0]^T$ and $[1, 2.5, 0]^T$) produced by the driving signals obtained in Section 4.2. The results in Figure 11 suggest that the dispersion of the frequency responses at the listening positions are stable within a range of 3 dB under a spatial Nyquist frequency of a linear array of about $f = 3.4$ kHz. The sound pressure levels at the quiet positions are lower about 30 dB than those at the listening positions.

Consequently, the results of these analyses suggest that the proposed system is efficient and stable for practical implementations.

5. Conclusions. To achieve local sound field propagation in the horizontal plane, this paper proposed an analytical approach based on dimension mismatches between 3-dimensional

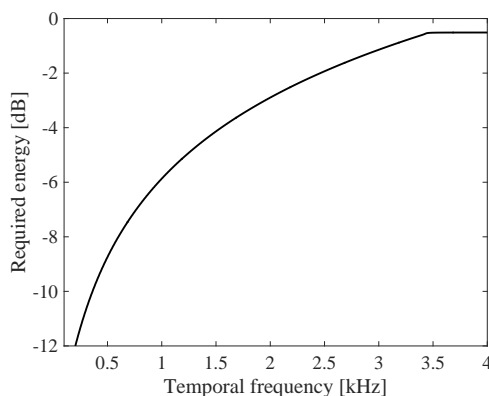


FIGURE 10. Results of required energy of a linear array of 64 loudspeakers for proposed method in comparison to monopole sound source defined in equation (17). Spatial Nyquist frequency is about 3.4 kHz.

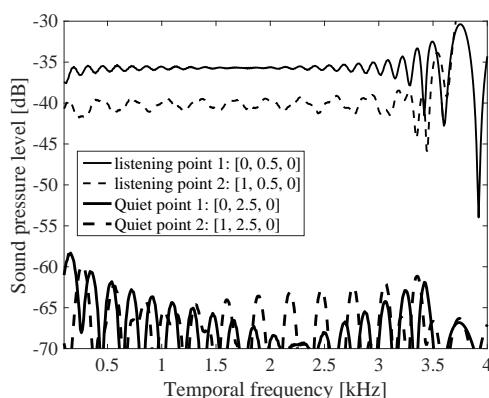


FIGURE 11. Results of synthesized sound pressure level at listening positions and quiet positions in proposed method with a linear array of 64 loudspeakers. Spatial Nyquist frequency is about 3.4 kHz.

point source propagation and 2.5-dimensional sound synthesis using a linear sound source. Two types of sound sources located close together are simultaneously produced in mutual opposite phase. The propagated sound pressure at the reference line is then completely cancelled, but the propagated sound pressure near the sound source is not compensated. An analytical method using a point source and a linear loudspeaker array was proposed. The driving functions of the point and linear sound sources and the resulting sound pressures were analytically derived and the radiation property was analyzed. The results of computer simulation showed that the proposed method can realize more effective local sound field propagation in the horizontal plane at all temporal frequencies than a simple monopole source and the evanescent wave production method. In addition, the discretization and truncation effects of the loudspeaker arrays, the radiation properties to the vertical angles, the stability of the driving signals, and the frequency responses of the produced sound field were also evaluated for actual implementations. These results suggest the practical aspect of the proposed method for multiple users of different heights.

To improve the proposed method, reducing radiation in the vertical direction, and synthesizing reverberant environments remain subjects for future work.

Appendix. Sound pressure at a position \mathbf{x} in the time domain $p(\mathbf{x}, t)$ is transformed to that in the temporal frequency domain $P(\mathbf{x}, \omega)$ by the temporal Fourier transform as

$$P(\mathbf{x}, \omega) = \int_{-\infty}^{\infty} p(\mathbf{x}, t) e^{-j\omega t} dt, \quad (18)$$

where $\omega = 2\pi f$ is the radiant frequency, $f = c/\lambda$ is the temporal frequency, c is the speed of sound, λ is the wavelength, t is the time and $j = \sqrt{-1}$.

Sound pressure in the wavenumber domain $\tilde{P}(k_x, y, z, \omega)$ is obtained from that in the temporal frequency domain $P(\mathbf{x}, \omega)$ from the spatial Fourier transform as

$$\tilde{P}(k_x, y, z, \omega) = \int_{-\infty}^{\infty} p(\mathbf{x}, \omega) e^{jk_x x} dx, \quad (19)$$

exemplarily for the x -dimension. $k = \omega/c$ is the wavenumber and k_x is the spatial frequency in the direction of x .

The according inverse Fourier transforms are obtained by changing the algebraic sign in the exponent and normalizing with $1/2\pi$.

Acknowledgment. This study was partly supported by JSPS KAKENHI Grant Numbers 25871208 and 15K21674.

REFERENCES

- [1] T. Okamoto, Generation of multiple sound zones by spatial filtering in wavenumber domain using a linear array of loudspeakers, *Proc. ICASSP*, May 2014, pp. 4733–4737.
- [2] T. Okamoto and A. Sakaguchi, Experimental validation of spatial Fourier transform-based multiple sound zone generation with a linear loudspeaker array, *J. Acoust. Soc. Am.*, vol. 141, no. 3, pp. 1769–1780, Mar. 2017.
- [3] T. Okamoto, Analytical methods of generating multiple sound zones for open and baffled circular loudspeaker arrays, *Proc. WASPAA*, Oct. 2015.
- [4] W. F. Druyvesteyn and J. Garas, Personal sound, *J. Audio Eng. Soc.*, vol. 45, no. 9, pp. 685–701, Sept. 1997.
- [5] J.-H. Chang, C.-H. Lee, J.-Y. Park, and Y.-H. Kim, A realization of sound focused personal audio system using acoustic contrast control, *J. Acoust. Soc. Am.*, vol. 125, no. 4, pp. 2091–2097, Apr. 2009.
- [6] S. J. Elliott, J. Cheer, J.-W. Choi, and Y. Kim, Robustness and regularization of personal audio systems, *IEEE Trans. Audio, Speech, Lang. Process.*, vol. 20, no. 7, pp. 2123–2133, Sept. 2012.
- [7] Y. Cai, M. Wu, and J. Yang, Sound reproduction in personal audio systems using the least-squares approach with acoustic contrast control constraint, *J. Acoust. Soc. Am.*, vol. 135, no. 2, pp. 734–741, Feb. 2014.
- [8] T. Betlehem, W. Zhang, M. Poletti, and T. Abhayapala, Personal sound zones: Delivering interface-free audio to multiple listeners, *IEEE Signal Process. Mag.*, vol. 32, no. 2, pp. 81–91, Mar. 2015.
- [9] M. A. Poletti and F. M. Fazi, An approach to generating two zones of silence with application to personal sound systems, *J. Acoust. Soc. Am.*, vol. 137, no. 2, pp. 598–605, Feb. 2015.
- [10] M. A. Poletti and F. M. Fazi, Generation of half-space sound fields with application to personal sound systems, *J. Acoust. Soc. Am.*, vol. 139, no. 3, pp. 1294–1302, Mar. 2016.
- [11] J.-W. Choi and Y.-H. Kim, Generation of an acoustically bright zone with an illuminated region using multiple sources, *J. Acoust. Soc. Am.*, vol. 111, no. 4, pp. 1695–1700, Apr. 2002.
- [12] M. Shin, S. Q. Lee, F. M. Fazi, P. A. Nelson, D. Kim, S. Wang, K. H. Park, and J. Seo, Maximization of acoustic energy difference between two spaces, *J. Acoust. Soc. Am.*, vol. 128, no. 1, pp. 121–131, July 2010.
- [13] P. Coleman, P. J. B. Jackson, M. Olik, M. Møller, M. Olsen, and J. A. Pedersen, Acoustic contrast, planarity and robustness of sound zone methods using a circular loudspeaker array, *J. Acoust. Soc. Am.*, vol. 135, no. 4, pp. 1929–1940, Apr. 2014.
- [14] Y. J. Wu and T. D. Abhayapala, Spatial multizone soundfield reproduction: Theory and design, *IEEE Trans. Audio, Speech, Lang. Process.*, vol. 19, no. 6, pp. 1711–1720, Aug. 2011.

- [15] N. Radmanesh and I. S. Burnett, Generation of isolated wideband sound fields using a combined two-stage Lasso-LS algorithm, *IEEE Trans. Audio, Speech, Lang. Process.*, vol. 21, no. 2, pp. 378–387, Feb. 2013.
- [16] W. Jin and W. B. Kleijn, Theory and design of multizone soundfield reproduction using sparse methods, *IEEE/ACM Trans. Audio, Speech, Lang. Process.*, vol. 23, no. 12, pp. 2343–2355, Dec. 2015.
- [17] N. Radmanesh, I. S. Burnett, and B. D. Rao, A Lasso-LS optimization with a frequency variable dictionary in a multizone sound system, *IEEE/ACM Trans. Audio, Speech, Lang. Process.*, vol. 24, no. 3, pp. 583–593, Mar. 2016.
- [18] W. Zhang, T. D. Abhayapala, T. Betlehem, and F. M. Fazi, Analysis and control of multi-zone sound field reproduction using modal-domain approach, *J. Acoust. Soc. Am.*, vol. 140, no. 3, pp. 2134–2144, Sept. 2016.
- [19] H. Itou, K. Furuya, and Y. Haneda, Evanescent wave reproduction using linear array of loudspeakers, *Proc. WASPAA*, Oct. 2011, pp. 37–40.
- [20] H. Itou, K. Furuya, and Y. Haneda, Localized sound reproduction using circular loudspeaker array based on acoustic evanescent wave, *Proc. ICASSP*, Mar. 2012, pp. 221–224.
- [21] J.-H. Chang and F. Jacobsen, Sound field control with a circular double-layer array of loudspeaker, *J. Acoust. Soc. Am.*, vol. 131, no. 6, pp. 4518–4525, June 2012.
- [22] J.-H. Chang and F. Jacobsen, Experimental validation of sound field control with a circular double-layer array of loudspeakers, *J. Acoust. Soc. Am.*, vol. 133, no. 4, pp. 2046–2054, Apr. 2013.
- [23] T. Okamoto, Near-field sound propagation based on a circular and linear array combination, *Proc. ICASSP*, Apr. 2015, pp. 624–628.
- [24] E. G. Williams, *Fourier Acoustics: Sound Radiation and Nearfield Acoustic Holography*. London, UK: Academic Press, 1999.
- [25] F. M. Fazi and P. A. Nelson, Nonuniqueness of the solution of the sound field reproduction problem with boundary pressure control, *Acta Acust. Acust.*, vol. 98, no. 1, pp. 1–14, Jan. 2012.
- [26] T. Okamoto, Analytical approach to 2.5D sound field control using a circular double-layer array of fixed-directivity loudspeakers, *Proc. ICASSP*, Mar. 2017, pp. 91–95.
- [27] S. Spors, R. Rabenstein, and J. Ahrens, The theory of wave field synthesis revisited, *Proc. 124th Conv. Audio Eng. Soc.*, May 2008.
- [28] J. Ahrens and S. Spors, Sound field reproduction using planar and linear arrays of loudspeakers, *IEEE Trans. Audio, Speech, Lang. Process.*, vol. 18, no. 8, pp. 2038–2050, Nov. 2010.
- [29] T. Okamoto, 2.5D higher-order Ambisonics for a sound field described by angular spectrum coefficients, *Proc. ICASSP*, Mar. 2016, pp. 326–330.
- [30] I. S. Gradshteyn and I. M. Ryzhik *Table of integrals, series, and products*. New York: Academic Press, 2007.
- [31] J. Ahrens and S. Spors, Reproduction of focused sources by the spectral division method, *Proc. ISCCSP*, Mar. 2010.
- [32] T. Okamoto, S. Enomoto, and R. Nishimura, Least squares approach in wavenumber domain for sound field recording and reproduction using multiple parallel linear arrays, *Appl. Acoust.*, vol. 86, pp. 95–103, Dec. 2014.